行政院國家科學委員會專題研究計畫 成果報告

新型二價銅離子化學偵測分子的合成及評估
研究成果報告(精簡版)

計 畫 類 別 ：個別型
計 畫 編 號 ：NSC 98-2113-M-009-006-
執 行 期 間 ：98 年 08 月 01 日至 99 年 07 月 31 日
執 行 單 位 ：國立交通大學應用化學系（所）

計 畫 主 持 人：吳淑祿

計畫參與人員：碩士班研究生-兼任助理人員：鐘健豪
碩士班研究生-兼任助理人員：許振宜
碩士班研究生-兼任助理人員：杜昆儒
博士班研究生-兼任助理人員：劉士榮
博士班研究生-兼任助理人員：M. Vedamal
博士班研究生-兼任助理人員：宋益銘

處 理 方 式 ：本計畫可公開查詢

中 華 民 國 99 年 10 月 28 日

The results of this project have been published in *Dalton Transactions*, 2010, ***39***, 4363 – 4368. The paper is listed below

Colorimetric Sensing of Cu(II): Cu(II) Induced Deprotonation of an Amide Responsible for Color Changes

Shu-pao Wu*, Kun-Ju Du and Yi-Ming Sung

Abstract

A 9,10-anthraquinone based chemosensor (chemosensor **1**) indicates the presence of Cu(II) ions among other transition metal ions with high selectivity through a color change from yellow to dark red. Chemosensor **2** shows binding with Cu(II), Ni(II) and Co(II) with color changes from yellow to dark red, red and pale green, respectively. In particular, Co(II) binding with chemosensor **2** causes significant green fluorescence. Upon addition of Cu(II), chemosensors **1** and **2** exhibit 76 nm and 80 nm red shifts in absorption wavelength (pH 7.0). The effect of the formation of these **1**–Cu(II) and **2**–Cu(II) complexes on pH was determined using Ultraviolet-visible spectroscopic pH titration. In the pH range of 6 - 7.5, a maximum absorption was observed at 473 nm and exhibited the formation of deprotonated **1**–Cu(II) and **2**–Cu(II) complexes.

Introduction

In recent years, an intense effort has been placed on the development of molecular devices for metal ion detection. The most common approach to the development of metal ion chemosensors is to connect a metal-binding unit with a signaling unit such as a chromophore or a fluorophore. The presence of metal ions causes a signal during interactions with binding units that results in a change in absorption wavelength or emission intensity.[1] A metal ion chemosensor can be viewed as a metal-binding ligand. Metal ion chemosensors can selectively bind a specific metal ion or have a higher binding affinity towards a metal ion.

Among the first row transition metal ions, Cu(II) and Zn(II) are two of the most frequently studied metal ions in the area of chemosensors.[2,3] Only a few chemosensors have been developed for Fe(III), Co(II) and Ni(II) due to their low binding affinity with a given ligand.[4,5] According to the Irving-Williams series, out of the first row transition metal ions, Cu(II) has the greatest formation constant with ligands containing oxygen or nitrogen donor atoms.[6] This is a great advantage when considering the design of Cu(II) chemosensors. To distinguish Cu(II) ions from other metal ions, a chemosensor must be designed with a suitable binding affinity toward metal ions. In the other words, a Cu(II) chemosensor is a “poor” ligand, which only binds Cu(II) ions or has a significantly higher binding affinity with Cu(II) ions than

with other metal ions.

Cu(II) recognition is also a key issue for the design of Cu(II) chemosensors. Cu(II) can induce deprotonation of the NH amide or NH groups that are conjugated to aromatic compounds upon Cu(II) binding. This deprotonation process caused by Cu(II) binding can be used for Cu(II) recognition. In addition, Cu(II)-induced deprotonation of NH groups that are conjugated to aromatic compounds, such as 1,4-naphthoquinone[2l] and 9,10-anthraquinone[2f,2g], cause an internal charge transfer (ICT), which can be observed as a shift in absorption wavelength or color change. This color change mechanism has recently been applied for highly selective Cu(II) detection.

In this study, two 9,10-anthraquinone based chemosensors (chemosensors **1** and **2,** see Scheme 1) were designed for metal ion detection. The 9,10-anthraquinone moiety has recently been used as a signal unit for sensing metal ions and anions because its optical properties can be significantly perturbed by chemical stimuli.[2f,2g,7,8] Both chemosensors contain an amide attached to a 9,10-anthraquinone moiety and function as chelating agents that are able to form complexes with metal ions. The only difference is the ring in the metal-chelating ligand: chemosensor **1** contains a benzene ring and chemosensor **2** contains a pyridine ring. This difference results in chemosensors **1** and **2** exhibiting different metal ion selectivity. Chemosensor **1** shows highly selective binding with Cu(II), resulting in a pronounced color change from yellow to red. Chemosensor **2** shows binding toward Cu(II), Ni(II) and Co(II) with a color change from yellow to dark red, red and pale green, respectively. In particular, Co(II) binding with chemosensor **2** causes significant green emission. The pH titration experiments on Cu(II) binding with chemosensors **1** and **2** revealed that the color change upon Cu(II) binding was primarily due to the deprotonation of the amide group attached to 9,10-anthraquinone.

Results and Discussion

Synthesis of Chemosensors 1 and 2

The procedure for the synthesis of chemosensor **1** and **2** is shown in Scheme 1. 1-(Chloroacetylamido)-anthracene-9,10-dione was reacted with benzyl amine or aminomethylpyridine to form chemosensors **1** and **2,** respectively. These products were purified using column chromatography with a 1:5 ethyl acetate:hexane eluent and subsequently characterized using mass and NMR spectrometry. The structures of chemosensors **1** and **2** are similar; the only difference is the ring in the metal-chelating ligand. Chemosensor **1** contains a benzene ring while chemosensor **2** contains a pyridine ring. Both chemosensors are yellow with a maximum absorption wavelength at 397 nm and exhibit weak fluorescence (λ_{em} = 505 nm, Φ = 0.002).

Spectrophotometric Estimation of Cu(II) Binding with Chemosensors 1 and 2

The ability of chemosensor **1** to form complexes with metal ions was first studied using Ultraviolet-visible (UV-vis) spectroscopy. Metal ions including Ca^{2+}, Cd^{2+}, Co^{2+}, Cu^{2+}, Fe^{2+}, Fe^{3+}, Hg^{2+}, Mg^{2+}, Mn^{2+}, Ni^{2+} and Zn^{2+} were tested using chemosensor **1** for ion detection. The UV-vis spectra resulting from the introduction of various metal ions are presented in Figure 1. For chemosensor **1**, Cu^{2+} was unique in producing a 76-nm red-shift (from 397 nm to 473 nm), which resulted in a visible color change from yellow to dark red (see Figure 1). Competitive experiments were carried out in the presence of Cu^{2+} with other metal ions (Figure 2). The absorption change at 473 nm caused by the mixture of Cu^{2+} with the other metal ion was similar to that caused by only Cu^{2+}. This indicates that other metal ions did not interfere with the binding of chemosensor **1** with Cu^{2+}. These observations indicate that Cu^{2+} is the only ion readily bound with chemosensor **1** to induce a color change from yellow to dark red, permitting highly selective detection of Cu^{2+}.

The ability of chemosensor **2** to form complexes with metal ions was also studied using UV-vis spectroscopy (Figure 3). The addition of Cu^{2+} to chemosensor **2** caused an 80-nm red-shift (from 397 nm to 477 nm), which resulted in a color change from yellow to dark red. This observation is similar to that of the addition of Cu^{2+} to chemosensor **1**. Cu^{2+} binding with chemosensors **1** and **2** caused an almost identical red-shift and color change. Addition of Ni^{2+} to chemosensor **2** caused an 86-nm red-shift (from 397 nm to 483 nm), which resulted in a color change from yellow to red (Figure 4). The addition of Co^{2+} to chemosensor **2** resulted in a blue-shift and a color change from yellow to pale green, resulting in significant green light emission (Figure 4). Chemosensor **2** shows less selective detection of metal ions, such as Cu^{2+}, Ni^{2+}, and Co^{2+}.

The ability of chemosensors **1** and **2** to form complexes with metal ions was also studied using fluorescence spectroscopy. For chemosensor **1**, Cu^{2+} was the only metal ion which resulted in significant fluorescence quenching (see Figure S1 in the supplementary data). Other metal ions only caused minor changes in fluorescence intensity. Chemosensor **1** detected Cu^{2+} through a fluorescence quenching process which arises from an energy or charge transfer mechanism[2k]. Co^{2+} binding with chemosensor **2** resulted in a significant increase in fluorescence intensity (Figure 5), while other metal ions only caused a small change in fluorescence intensity. The quantum yield of **2**-Co^{2+} complexes was determined as 0.242, which is 100-fold higher than that of chemosensor **2**, at 0.002. This demonstrated that chemosensor **2** can detect Co^{2+}, yielding a significant increase in fluorescence. The mechanism of fluorescence of **2**-Co^{2+} complexes is based on CHEF (chelation-enhanced fluorescence) of 1-amino-9,10-anthraquinone[9]. Competitive experiments were carried

out in the presence of Co^{2+} with other metal ions (Figure 6). Emission intensity at 520 nm caused by Co^{2+} was completely quenched in the presence of Cu^{2+}. This indicates that Cu^{2+} dominated binding with chemosensor **2** and resulted in low emission intensity. In the presence of Ni^{2+}, emission intensity reached half the intensity of Co^{2+}-**2** complexes. This observation indicates that Ni^{2+} and Co^{2+} competed to bind with chemosensor **2**. In addition, the colors of the metal ion mixture with chemosensor **2** depended on the composition. In the presence of Cu^{2+}, the color was dark red and no green light emission was observed. In the presence of Ni^{2+}, the color was red and weak green light emission was observed. These findings indicated that Cu^{2+} dominates binding with chemosensor **2** followed by Ni^{2+}. This observation is consistent with the Irving-Williams series, in which Cu(II) has the highest formation constant with ligands among the first row transition metal ions.

Stoichiometries and Affinity Constants of 1-Cu^{2+} and 2-Cu^{2+}

The binding stoichiometry of **1**-Cu^{2+} and **2**-Cu^{2+} complexes was determined using Job's plot experiments[10]. In Figure 7, the absorbance at 473 nm was plotted against the molar fraction of both chemosensors under a constant total concentration. A maximum absorbance was observed when the molar fraction was 0.5, which indicates a 1:1 ratio for both the **1**-Cu^{2+} and **2**-Cu^{2+} complexes. The association constant, K_a, was evaluated graphically by plotting $1/\Delta A$ against $1/[Cu^{2+}]$ as shown in Figure 8. The data was linearly fit according to the Benesi-Hilderbrand equation and a K_a value was obtained from the slope and intercept of the line.[9] The K_a values obtained for **1**-Cu^{2+} and **2**-Cu^{2+} complexes were 8470 M^{-1} and 18667 M^{-1}, respectively. For Cu^{2+} binding, chemosensor **2** has a two-fold higher association constant than chemosensor **1**. This is due to the extra coordination nitrogen in the pyridine ring. The binding stoichiometry of the **2**-Ni^{2+} and **2**-Co^{2+} complexes was also determined using Job's plot experiments (Figure 9). The **2**-Ni^{2+} complex has a maximum point at 0.6, which indicates two possible ratios (**2**/Ni^{2+}), 1:1 and 2:1. The **2**-Co^{2+} complex has a maximum point at 0.4, which indicates two possible ratios (**2**/Co^{2+}), 1:1 and 1:2, for **2**-Co^{2+} complexes.

To demonstrate the Cu^{2+}-induced deprotonation of the amide group in chemosensor **1**, pH titration experiments were carried out. First, the influence of pH on chemosensor **1** was studied using UV-vis spectroscopy (see Figure S2 in the supplementary information). Over a pH range of 6 - 10, the visible absorption band centered at 397 nm was unchanged. A decrease in pH from 5.5 to 1 engendered a shift in the maximum absorption wavelength to 390 nm; this 7-nm shift was due to protonation of the amide group. The effect of pH on Cu^{2+} binding to chemosensor **1** was further studied by monitoring red **1**-Cu^{2+} complexes at a wavelength of 473 nm (see Figure 10). The absorbance at this wavelength suddenly increased at pH 6.0 and reached a maximum over a pH range of 6.0 - 7.5 for chemosensor **1**. This indicates

that the formation of red **1**-Cu^{2+} complexes is a deprotonation process. When the pH value exceeded 8, the absorbance at 473 nm gradually decreased. This was due to the dissociation of red **1**-Cu^{2+} complexes, which resulted in lower absorbance at 473 nm. At pH values less than 4 absorbance was almost negligible; evidently the **1**-Cu^{2+} complexes do not exist over this pH range. For chemosensor **2**, there were two flat areas in the pH range of 3.5 - 5.5 and 6.0 - 10.0. The first flat area (pH 3.5 - 5.5) indicated the formation of non-deprotonated **2**-Cu^{2+} complexes. The second flat area (pH 6.0 - 10.0) represented the formation of deprotonated **2**-Cu^{2+} complexes. This observation differed from that of chemosensor **1**. The deprotonated **1**-Cu^{2+} complexes were gradually decomposed at pH > 8, but the deprotonated **2**-Cu^{2+} complexes were stable at pH > 8.

The effect of pH on the formation of **2**-Ni^{2+} and **2**-Co^{2+} complexes was also studied (see Figure S3 in the supplementary information). For **2**-Ni^{2+} complexes, the absorbance at the wavelength 479 nm abruptly increased at pH 6.0 and reached a maximum at pH 8.0. This indicates that the formation of red **2**-Ni^{2+} complexes is a deprotonation process. When the pH value exceeded 8, the absorbance at 479 nm gradually decreased, due to the dissociation of red **2**-Ni^{2+} complexes. For the **2**-Co^{2+} complexes, the emission at the wavelength 520 nm increased sharply at pH 6.5, and reached a maximum at pH 7.5. This also indicates that the formation of **2**-Co^{2+} complexes is a deprotonation process.

To gain a clearer understanding of the structure of **1**-Cu^{2+} complexes, Infrared (IR) spectroscopy was employed. The IR spectra were primarily characterized by bands in the carbonyl region. Two bands, 1666 cm^{-1} and 1652 cm^{-1}, were associated with C=O absorption in the amide and quinone components of chemosensor **1** (see Figure S4 in the supplementary information). Binding of Cu^{2+} with chemosensor **1** resulted in a shift in the carbonyl region peaks to 1660 cm^{-1} and 1626 cm^{-1}. The significant shift observed in the carbonyl absorption band from 1652 cm^{-1} to 1626 cm^{-1} was due to Cu^{2+} induced deprotonation of the amide group during binding.[11] The downward shift in the IR spectrum from 1666 cm^{-1} to 1660 cm^{-1} was indicative of direct interaction between Cu^{2+} and the anthrance-9,10-dione oxygen.[12] Chemosensor **1** thus forms a tridentate ligand in which Cu^{2+} is bound with two nitrogens and one oxygen in anthraquinone. This model is consistent with previous indications that Cu^{2+} ions form a 1:1 ratio complex with chemosensor **1** (Scheme 2). The IR spectra of **2**-Cu^{2+} complexes is similar to that of **1**-Cu^{2+} complexes. Binding of Cu^{2+} with chemosensor **2** resulted in a shift in the carbonyl region from 1651 cm^{-1} to 1645 cm^{-1} and from 1679 cm^{-1} to 1670 cm^{-1}. This indicated that Cu^{2+} bonded with chemosensor **2** through the carbonyl oxygen in anthraquinone.

Conclusions

In summary, two 9,10-anthraquinone based colorimetric chemosensors have been developed for Cu^{2+} detection. Chemosensor **1** functions as a chelating agent that binds a Cu^{2+} ion through three functional groups: amine nitrogen, amide nitrogen and quinone oxygen. The Cu^{2+} binding of chemosensor **1** induces deprotonation of the amide group and results in a significant color change from yellow to dark red, with a 76-nm red-shift. Chemosensor **2** can detect Cu(II), Ni(II) and Co(II) with a color change from yellow to dark red, red and pale green, respectively. In particular, Co(II) binding with chemosensor **2** causes significantly green fluorescence.

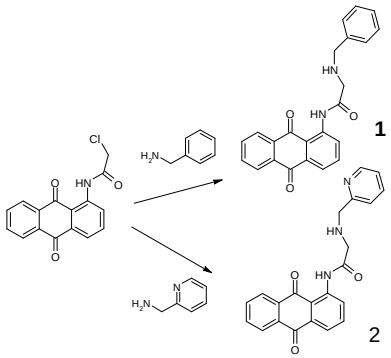

Scheme 1. Synthesis of chemosensors **1** and **2**.

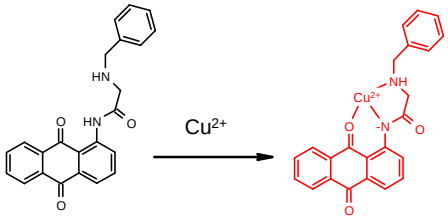

Scheme 2. A bonding model of the **1**-Cu^{2+} complex.

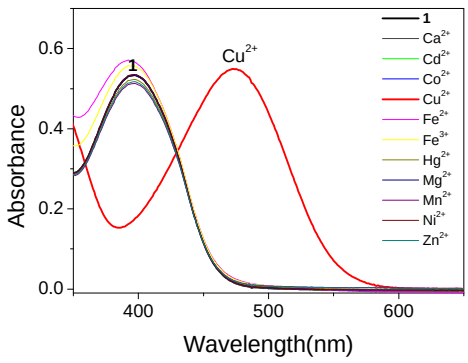

1 **1+Co^{2+}** **1+Cu^{2+}** **1+Ni^{2+}**

Figure 1. (Top) Absorption change in the UV-vis spectra of chemosensor **1** (black line, 100 μM) upon the addition of metal ions (100 μM) in a methanol-H_2O solution (v/v = 4/1, 20 mM Hepes buffer, pH 7.0). (Bottom) Color of chemosensor **1** (100 μM) before and after the addition of metal ions (100 μM) in a methanol-H_2O solution (v/v = 4/1, 20 mM Hepes buffer, pH 7.0).

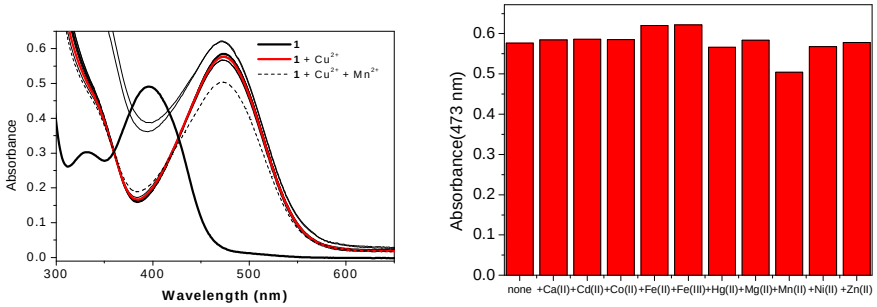

Figure 2. (right) UV-vis absorption response of chemosensor **1** (black line, 100 μM) to Cu^{2+}(200 μM) over the selected metal ions (200 μM) in a methanol-H_2O solution (v/v = 4/1, 20 mM Hepes buffer, pH 7.0). (left) Absorbance at 473 nm upon the addition of chemosensor **1** to Cu^{2+} over the selected metal ions.

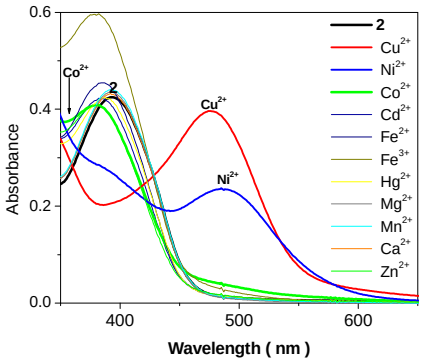

Figure 3. Absorption change in the UV-vis spectra of chemosensor **2** (black line, 100 μM) upon the addition of metal ions (100 μM) in a methanol-H_2O solution (v/v = 4/1, 20 mM Hepes buffer, pH 7.0).

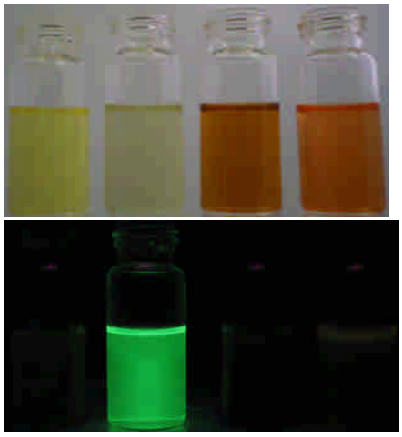

2 **2+Co^{2+}** **2+Cu^{2+}** **2+Ni^{2+}**

Figure 4. Color (top) and fluorescence (bottom) of chemosensor **2** (100 μM) before and after the addition of metal ions (100 μM) in a methanol-H_2O solution (v/v = 4/1, 20 mM Hepes buffer, pH 7.0).

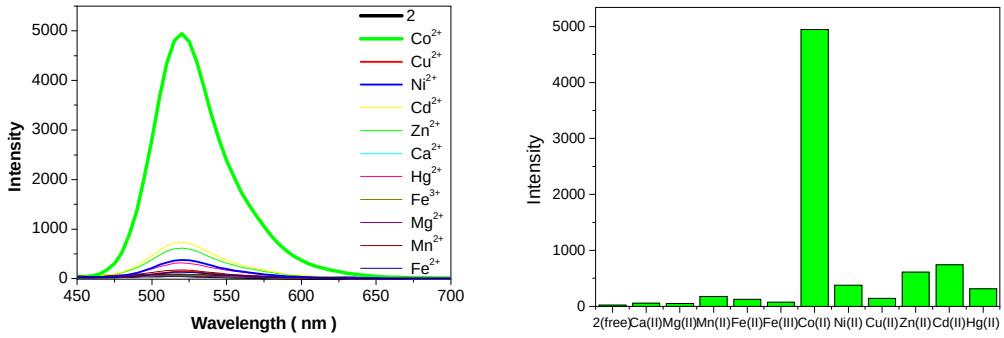

Figure 5. (right) Fluorescence spectra of chemosensor **2** (100 μM) in a methanol-H_2O solution (v/v = 4/1, 20 mM Hepes buffer, pH 7.0) in the presence of different metal ions (100 μM). (left) Emission intensity at 520 nm of chemosensor **2** in the presence of different metal ions

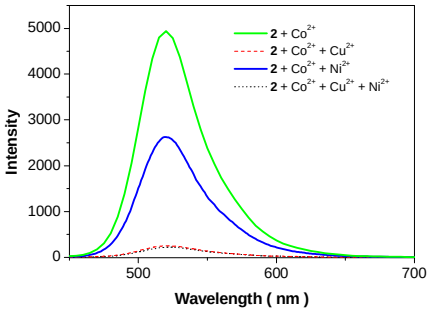

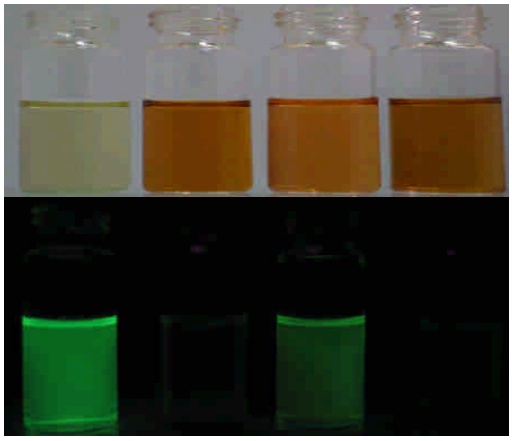

Co^{2+}	+	+	+	+
Ni^{2+}	−	−	+	+
Cu^{2+}	−	+	−	+

Figure 6. (right) Fluorescence spectra of chemosensor **2** (100 μM) after the addition of metal ions (200 μM) in a methanol-H_2O solution (v/v = 4/1, 20 mM buffer). (Bottom) Color and emission of chemosensor **2** after the addition of anions.

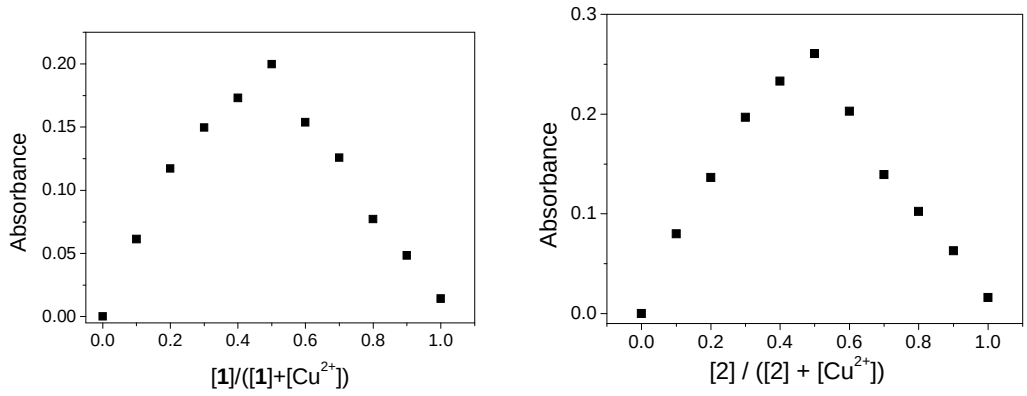

Figure 7. Job's plot of a 1:1 complex of **1**-Cu^{2+} (right) and **2**-Cu^{2+} (left), where the absorbance at 473 nm was plotted against the mole fraction of Cu^{2+} at a constant total concentration of 1.0×10^{-4} M in a methanol-H_2O solution (v/v = 4/1, 20 mM Hepes buffer, pH 7.0).

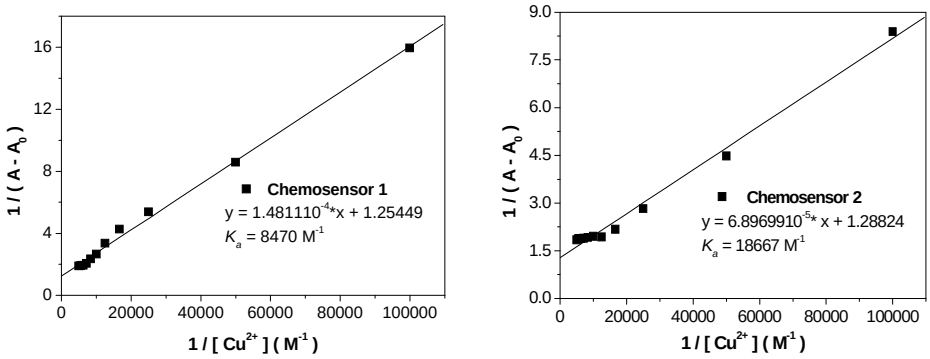

Figure 8. Benesi-Hilderbrand plot of chemosensor **1** (right) and chemosensor **2** (left) with $Cu(BF_4)_2$.

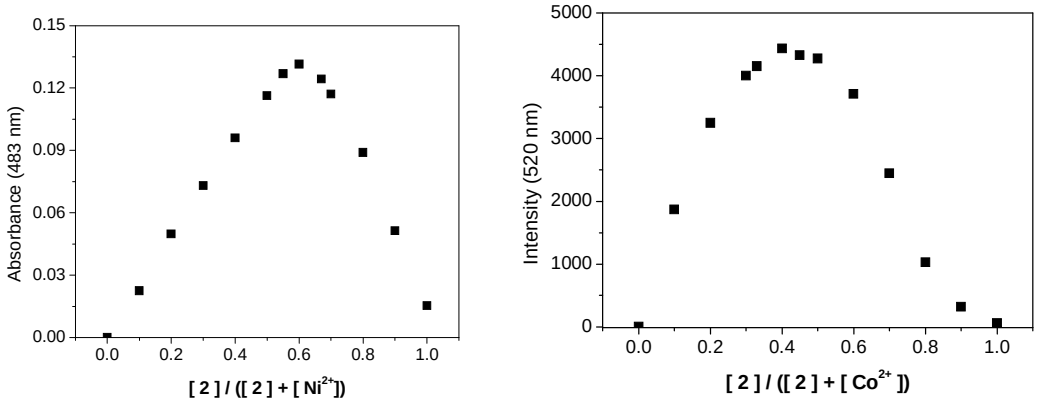

Figure 9. Job's plot of **2**-Ni^{2+} (right) and **2**-Co^{2+} (left) complexes, where the absorbance at 483 nm (**2**-Ni^{2+}) or the fluorescence at 520 nm (**2**-Co^{2+}) was plotted against the mole fraction of Ni^{2+} or Co^{2+} at a constant total concentration of 1.0×10^{-4} M in a methanol-H_2O solution (v/v = 4/1, 20 mM Hepes buffer, pH 7.0).

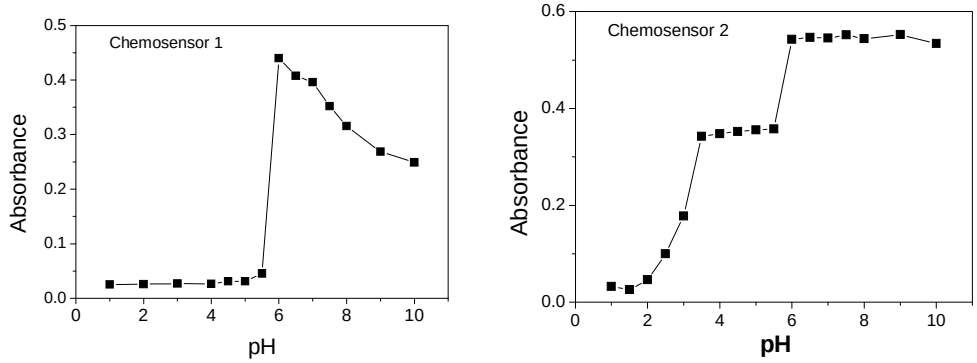

Figure 10. pH titration of Cu^{2+} (10^{-4} M) bonded with chemosensor **1** (right) and chemosensor **2** (left) (10^{-4} M) in a methanol-H_2O solution (v/v = 4/1, 20 mM buffer). The absorbance at 473 nm was plotted against pH.

無衍生研發成果推廣資料

98 年度專題研究計畫研究成果彙整表

計畫主持人：吳淑祿	計畫編號：98-2113-M-009-006-
計畫名稱：新型二價銅離子化學偵測分子的合成及評估	

成果項目			量化			單位	備註（質化說明：如數個計畫共同成果、成果列為該期刊之封面故事...等）
			實際已達成數（被接受或已發表）	預期總達成數(含實際已達成數)	本計畫實際貢獻百分比		
國內	論文著作	期刊論文	0	0	100%	篇	
		研究報告/技術報告	0	0	100%		
		研討會論文	0	0	100%		
		專書	0	0	100%		
	專利	申請中件數	0	0	100%	件	
		已獲得件數	0	0	100%		
	技術移轉	件數	0	0	100%	件	
		權利金	0	0	100%	千元	
	參與計畫人力（本國籍）	碩士生	0	0	100%	人次	
		博士生	0	0	100%		
		博士後研究員	0	0	100%		
		專任助理	0	0	100%		
國外	論文著作	期刊論文	2	2	100%	篇	
		研究報告/技術報告	0	0	100%		
		研討會論文	0	0	100%		
		專書	0	0	100%	章/本	
	專利	申請中件數	0	0	100%	件	
		已獲得件數	0	0	100%		
	技術移轉	件數	0	0	100%	件	
		權利金	0	0	100%	千元	
	參與計畫人力（外國籍）	碩士生	4	4	100%	人次	
		博士生	4	4	100%		
		博士後研究員	0	0	100%		
		專任助理	0	0	100%		

其他成果 (無法以量化表達之成果如辦理學術活動、獲得獎項、重要國際合作、研究成果國際影響力及其他協助產業技術發展之具體效益事項等，請以文字敘述填列。)	無

	成果項目	量化	名稱或內容性質簡述
科教處計畫加填項目	測驗工具(含質性與量性)	0	
	課程/模組	0	
	電腦及網路系統或工具	0	
	教材	0	
	舉辦之活動/競賽	0	
	研討會/工作坊	0	
	電子報、網站	0	
	計畫成果推廣之參與（閱聽）人數	0	

國科會補助專題研究計畫成果報告自評表

請就研究內容與原計畫相符程度、達成預期目標情況、研究成果之學術或應用價值（簡要敘述成果所代表之意義、價值、影響或進一步發展之可能性）、是否適合在學術期刊發表或申請專利、主要發現或其他有關價值等，作一綜合評估。

1. 請就研究內容與原計畫相符程度、達成預期目標情況作一綜合評估

■達成目標

□未達成目標（請說明，以 100 字為限）

□實驗失敗

□因故實驗中斷

□其他原因

說明：

2. 研究成果在學術期刊發表或申請專利等情形：

論文：■已發表 □未發表之文稿 □撰寫中 □無

專利：□已獲得 □申請中 ■無

技轉：□已技轉 □洽談中 ■無

其他：(以 100 字為限)

3. 請依學術成就、技術創新、社會影響等方面，評估研究成果之學術或應用價值（簡要敘述成果所代表之意義、價值、影響或進一步發展之可能性）(以 500 字為限）

主要研究貢獻，在於開發新穎金屬離子化學偵測分子，來偵測銅離子及鐵離子，並應用於環境中的金屬離子分析及觀測生物細胞中金屬離子的輸送及調節。於金屬離子化學偵測分子的研究領域，已經有優異及領先的研究成果.